Transverse-Wake Wave Breaking

S. V. Bulanov,[1,3] F. Pegoraro,[1] A. M. Pukhov,[2,*] and A. S. Sakharov[3]

[1]*Dipartimento di Fisica Teorica, Università di Torino, Torino, Italy*
[2]*Max-Planck-Institute for Quantum Optics, Garching bei Munchen, Germany*
[3]*General Physics Institute Russian Academy of Sciences, Moscow, Russia*

A finite-width laser pulse of high intensity propagating in an underdense plasma excites a transversely inhomogeneous, finite amplitude wakefield. This wake wave undergoes a transverse wave breaking due to the increase of the wake front curvature, followed by the self-intersection of electron trajectories. Transverse break occurs at much lower wave amplitudes than the conventional one-dimensional wave break. The resulting structures have generic forms that can be described by modified curves parallel to a parabola. Simulations with the particle-in-cell electromagnetic relativistic code VLPL2D show such structures appearing. [S0031-9007(97)03285-7]

Charged particle accelerators that use the ultrastrong electric field of a plasma wave driven in an underdense plasma by modern tabletop multiterawatt lasers [1] have been studied theoretically [2], experimentally [3], and numerically [4–6]. The wave is excited in the wake behind a short pulse [2] or develops as a result of laser-plasma instabilities [5,7]. The main goal of all such accelerators is to reach the largest possible accelerating field. A natural limit is given by wave breaking which, in a cold plasma and in the one-dimensional (1D) approximation, gives [8] $E_m = (mc\omega_{pe}/e)[2(\gamma_{ph} - 1)]^{1/2}$, with $\gamma_{ph} \equiv (1 - \beta_{ph}^2)^{-1/2} \approx \omega/\omega_{pe}$, $\beta_{ph} \equiv v_{ph}/c$, and v_{ph} the plasma wave phase velocity which is equal to the pulse group velocity. The break appears when the electron displacement in the wave is of the order of its wavelength. Even in a 1D geometry, the wave break takes different forms and appears either as a crash similar to that of a gravity wave at the sea shore, in which case the wave disappears, or, if it occurs adiabatically, as a sharp crest on the wave top. The latter regime in the plasma case means that only relatively few electrons leave the plasma wave. These fast electrons can enter the acceleration phase of the wakefield [9,10]. The breaking of the plasma wave, generated by forward stimulated Raman scattering of the laser radiation, leads to effective electron acceleration, as seen in particle-in-cell (PIC) simulations [5–7], and is thought to be the basic mechanism of fast electron production in the experiments presented in Ref. [3] (see discussion in Ref. [11]). Since the largest accelerating fields occur in strongly nonlinear plasma waves, the wave-breaking conditions and the typical structure of the break are of great interest for wakefield accelerators. In addition, the study of the wave-break structure is of general interest for nonlinear physics.

The process of wave breaking in 2D and 3D plasma waves is expected to exhibit more complicated properties [12]. A 2D wakefield plasma wave excited by a finite width, short laser pulse, or by a pulse with a sharp leading edge in an underdense plasma has a specific "horseshoe"

[6] (or "D shape") structure where the curvature of the constant phase surfaces increases with the distance from the pulse. The curvature radius R decreases until it is comparable to the electron displacement ξ in the nonlinear plasma wave leading to a new type of self-intersection of the electron trajectories. The resulting destruction of the regular structure of the wave can be invoked to explain the decay of the wakefield plasma wave observed in 2D simulations.

The goal of the present Letter is to describe the mechanism and the structure of a 2D break and to derive from it an estimate of the number of regular (i.e., not broken) wakefield periods behind the laser pulse. We consider a wakefield plasma wave excited by a laser pulse of finite width S driven "resonantly" by a pulse with length equal to or shorter than the plasma wavelength or by a pulse with a sharp leading front. The resonance condition gives $\omega_l/k_l = v_g$, where v_g is the pulse group velocity and ω_l and k_l are the local plasma wave frequency and wave vector that can be transversely inhomogeneous. The transverse nonuniformity of ω_l is caused by the inhomogeneity of the plasma density, if the laser pulse is guided in a plasma channel [13], by the relativistic dependence of ω_l on the plasma wave amplitude, which is determined by the pulse transverse shape, and by the pulse generated magnetic field, the magnitude of which vanishes along the axis and increases in the transverse direction as shown in the simulations presented in Refs. [4,14–16]. In the presence of a transverse magnetic field the frequency of the longitudinal plasma oscillations $\omega_l = (\omega_{pe}^2 + \omega_{Be}^2)^{1/2}$, with ω_{pe} the plasma frequency and ω_{Be} the cyclotron frequency. The general dependence of the plasma wave frequency on the transverse coordinate y can be approximated in the vicinity of the axis by the parabolic form $\omega_l(y) \approx \omega_l(0) + \Delta\omega_l(y/S)^2$. For a pulse guided in a channel, $\Delta\omega_l$ is the difference between the plasma frequency outside and inside the channel. For an ultrahigh intensity pulse, $a \equiv eA_\perp/mc^2 \gg 1$,

with transverse profile $a(y) = a(0)(1 - y^2/S^2)$, we have $\Delta\omega_l \approx \omega_l(0) = \pi\omega_p/[2a(0)]$. Here ω_p is the nonrelativistic plasma frequency and $A_\perp$ is the radiation vector potential. The transverse nonuniformity ω_l means that also the plasma wake wavelength $\lambda_l = 2\pi/k_l$ depends on y and that the phase surfaces are curved. The expression of the constant phase surfaces, $\psi(x, y) = \omega_l(y)(t - x/v_{\text{ph}}) = \text{const}$, shows that their curvature $1/R$ increases linearly with the distance L from the laser pulse, $1/R = 2L\Delta\omega_l/\omega_l(0)S^2$, where $L \equiv \psi v_{\text{ph}}/\omega_l(0)$. Integer values of $L\omega_l(0)/2\pi v_{\text{ph}}$ correspond to the number of wake plasma wave periods behind the pulse. Thus we can write the constant phase surfaces as $x_0 \equiv x - v_{\text{ph}}t + \psi v_{\text{ph}}/\omega_l(0) = y_0^2/2R$.

In a nonlinear plasma wave the real position of the constant phase surfaces is shifted from the surface given above by the oscillation amplitude $\xi(y_0)$. Thus, when curvature radius R becomes of the order of the electron displacement ξ, the wake plasma wave starts to break transversely. From these considerations, the distance between the laser pulse and the first place of breaking can be estimated as $\omega_l(0)S^2/2\Delta\omega_l\xi$, and the number of the regular wake wave periods as $\omega_l^2 S^2/4\pi c\Delta\omega_l\xi$. The exact form and spatial dependence of the displacement ξ in a 2D (or 3D) configuration depends on the specific laser plasma regime under consideration. In addition, the presence of an inhomogeneous quasistatic magnetic field influences the oscillations. In the following, for the sake of simplicity, we suppose ξ to be perpendicular to the parabolic phase surfaces derived in the linear approximation. As noted below, this assumption is not critical as long as the orientation of the displacement does not deviate too strongly from the normal. Then we can write the shifted surface as

$$x = x_0 + \xi(y_0)R/(R^2 + y_0^2)^{1/2},$$
$$y = y_0 - \xi(y_0)y_0/(R^2 + y_0^2)^{1/2}, \quad (1)$$
$$x_0 = y_0^2/2R.$$

If we simply neglect the dependence of the displacement $\xi(y_0)$ on the coordinate y_0 along the wave front, Eq. (1) defines a curve parallel to a parabola [17]. The singularity which is formed for $R \leq \xi$ corresponds to the self-intersection of the electron trajectories. Near this singularity the dependence of x on y is of the form $y \approx |x|^{3/4}$ (see, e.g., [18]). For $R < \xi$ a multivalued structure appears, i.e., the wave breaks. The constant phase curves $y(x)$ for three different values of the ratio ξ/R are shown in Fig. 1(a). The curve on the right of the figure, $\xi/R = 0.84$, still resembles a parabola, the central curve is taken close to the transverse wave-break condition and shows a sharp joint at $x = 0$, while the curve on the left, $\xi/R = 2.1$, is known as the "swallowtail" [18] in catastrophe theory. We notice here that catastrophe theory suggests which structurally stable wave-breaking regimes can occur [18], i.e., which structures are robust against changes in the exact form of the displacement ξ. Near the breaking
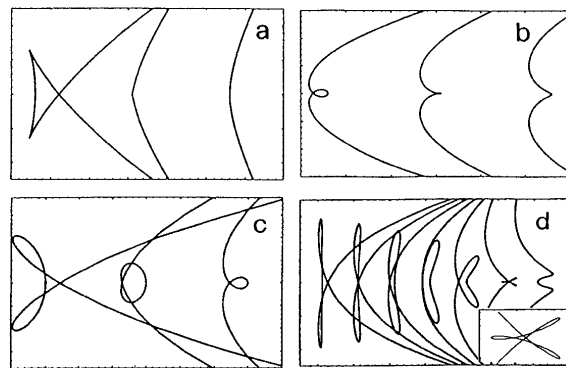
FIG. 1. Development of the transverse wave breaking. Constant phase curves $y = y(x)$ are shown for increasing ξ/R from left to right and for different y dependences of the displacement ξ, with R the curvature radius: (a) Formation of the swallowtail when ξ does not depend on y ($\xi/R = 0.84$, 1.05, 2.1); (b) formation of the loop when ξ has a Lorentzian form [$\xi(0)/R = 0.8$, 1, 1.3, $\delta = 1.5$, 1, 0.6]; (c) change of the type of singularity as ξ/R increases above threshold [$\xi(0)/R = 1.25$, 2.5, 5]; (d) evolution of the butterfly into a swallowtail-type structure when ξ has a sharp off-axis maximum [$\xi(0)/R = n/2$, $n = 1, \ldots, 6$].

threshold, the displacement is close in value to the curvature radius, $\xi/R - 1 = \varepsilon \ll 1$, and the size of the swallowtail is of order $\varepsilon^2 R$ along x and $\varepsilon^{3/2}R$ along y. The typical portion of the initial parabola affected by the break is given by $|y_0| < \varepsilon^{1/2}R$.

In a more realistic analysis, the amplitude of the displacement is not constant and in the most likely conditions it has its maximum at the axis. We describe this dependence with the Lorentzian form: $\xi(y_0) = \xi(0)/[1 + \delta(y_0/R)^2]$, where $\delta \approx (R/S)^2$. Close to the threshold, when $\varepsilon < 4\delta$, the type of the singularity changes as shown in Fig. 1(b) for values, from right to left, of ξ/R below, at and, respectively, above the transverse wave-break condition. At the wave-breaking threshold, the singularity is described by the generic semicubic form $x \approx |y|^{2/3}$, which corresponds to the cusp catastrophe [18]. For $\varepsilon = \xi(0)/R - 1$ well above the breaking threshold, we have $\varepsilon \approx 4\pi\xi\Delta\omega_l/\omega_l(0)k_lS^2 \gg 1$ while $\delta \approx (\xi/S)^2$. Then $\varepsilon > 4\delta$ and from Eq. (1) it follows that the singularity shown in Fig. 1(a) is realized. For these large values of ξ we see the formation of a loop on the inner side of the parabola changing into the swallowtail-type breaking as the ratio ξ/R increases. This transition is shown in Fig. 1(c). An additional structure of interest, the so-called "butterfly" shown in Fig. 1(d), corresponds to a displacement ξ with a local minimum on the axis and two sharp off-axis maxima. Such a displacement could be realized in cylindrical geometry in an annular pulse with its maximum amplitude at a distance from its axis. In addition, off-axis structures can be relevant to large amplitude pulses propagating in a plasma with $\omega_{\text{pe}}/\omega$ approaching unity, in which case a large quasistatic magnetic field that has its maximum amplitude off axis is generated.

In all these model representations of the transverse wave break, the displacement ξ is much smaller than the wavelength of the wakefield λ_l, and electron trajectories self-intersect mainly in the transverse direction. Nevertheless, when $\xi > (2\lambda_l R)^{1/2}$ some electrons can enter the accelerating electric field region from the transverse direction and can be accelerated along the direction of the laser pulse. This provides an effective mechanism for injecting a relatively small fraction of electrons into the acceleration region.

The occurrence of transverse wave breaking has been observed in a series of simulations with the two-dimensional version of the PIC electromagnetic relativistic code VLPL (Virtual Laser-Plasma Laboratory) developed at MPQ, Garching. Linearly polarized pulses with dimensionless amplitudes in the range $a = 4$ to 1.5 have been considered propagating, along x, in an underdense plasma with ω_{pe}/ω in the range 0.009 to 0.15. The pulse length has been varied accordingly, from 8λ to 60λ, and different width to length ratios have been considered in order to verify the scaling of the number of periods with the square of the transverse size S. These runs have explored different values of the ratio between ξ and R (and $2\pi/k_l$) corresponding to different regimes of transverse wave break, all characterized by the formation of structures of the type described above. The numerical results obtained for $a = 2.5$, $\omega_{pe} = 0.075\omega$, length 20λ, and width 26λ are shown in Figs. 2 and 3 at $\omega t/2\pi = 175$. The plasma wave closest to the pulse is not broken while the second wake plasma wave has undergone transverse wave break (along y). As can be seen from p_y, y phase space in Fig. 3(a), some electrons acquire large transverse momenta $p_y < 10mc$. They move toward the axis, where their trajectories self-intersect, and cause the multistream motion shown in Fig. 3(a) (see also the discussion in Ref. [11] of the observation of electrons moving transversely to the laser pulse axis in the laser wake field accelerator experiments). A numerical reconstruction of the spatial structure of the plasma displacement (not presented here) shows that the assumption that the displacement is nearly perpendicular to the phase surfaces is essentially correct before multistream motion appears after the wave break. The inward breaking in the transverse direction explains why the formation of evacuated channels was not observed in our simulation of the relativistic self-focusing [6]. In Fig. 2(b) the electron density distribution, which marks the position of the constant phase surfaces, displays, in correspondence with

FIG. 2. Structure of the break in the (x, y) plane behind a pulse with amplitude $a = 2.5$, width 26λ, and length 20λ in a plasma with $\omega/\omega_{pe} = 13$ for $\omega t/2\pi = 175$: (a) Electromagnetic energy density; (b) electron density marking the constant phase surfaces of the wake wave; (c) longitudinal electric field on the axis versus x; (d) (p_x, x) phase space integrated along y.
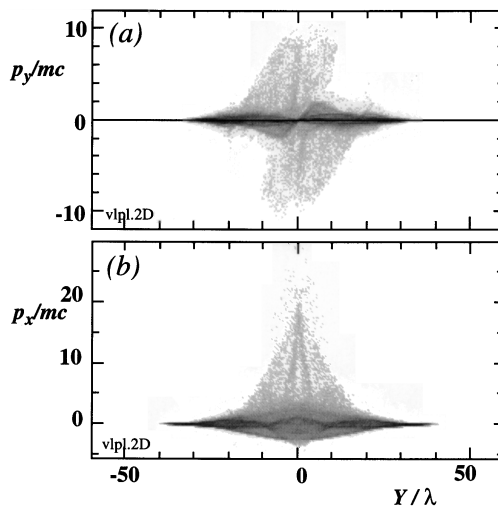
FIG. 3. (a) (p_y, y) phase space, and (b) (p_x, y) phase space integrated along x.

the second wake, a swallowtail structure that becomes more blurred in the third wave as a consequence of the intersection of the electron trajectories. The dependence of the longitudinal electric field on x in Fig. 2(c) shows that transverse wave break decreases its value and partly spoils its regular structure. By comparing the phase spaces (p_x, x) in Fig. 2(d) and (p_x, y) in Fig. 3(b) we see that the fast electrons, localized inside a narrow region on the axis, are accelerated in the swallowtail up to $p_x < 20mc$.

In conclusion, a new scenario for the plasma wave break has been presented that predicts both the location and the structure of the break. These features are generic and thus are relevant to a broad range of regimes of nonlinear wave evolution. In the wakefield plasma wave, only a relatively small part of the wave is involved in the 2D wave break, some electrons are injected into the accelerating portion of phase space and move in the longitudinal direction, while others are thrown aside. This regime can lead to the acceleration of fast particles, although in an uncontrolled way. The results of this Letter are also relevant to plasma wakefield accelerators driven by relativistic electron bunches, as the field excited by a finite size bunch exhibits similar properties.

---

[1] M. D. Perry and G. Mourou, Science **264**, 917 (1994).

[2] T. Tajima and J. M. Dawson, Phys. Rev. Lett. **43**, 267 (1979).

[3] A. Modena *et al.,* Nature (London) **337**, 606 (1995); K. Nakajima *et al.,* Phys. Rev. Lett. **74**, 4428 (1995).

[4] D. W. Forslund *et al.,* Phys. Rev. Lett. **54**, 558 (1985).

[5] C. D. Decker, W. Mori, and T. Katsouleas, Phys. Rev. E **50**, R3338 (1994).

[6] S. V. Bulanov, F. Pegoraro, and A. M. Pukhov, Phys. Rev. Lett. **74**, 710 (1995).

[7] S. V. Bulanov *et al.,* Phys. Fluids B **4**, 1935 (1992).

[8] A. I. Akhiezer and R. V. Polovin, JETP **3**, 696 (1956); T. Katsouleas and W. Mori, Phys. Rev. Lett. **61**, 90 (1988); E. Esarey and M. Pilloff, Phys. Plasmas **2**, 1432 (1995).

[9] S. V. Bulanov *et al.,* Sov. J. Plasma Phys. **16**, 444 (1990).

[10] D. Umstadter, J. M. Kim, and E. Dodd, Phys. Rev. Lett. **76**, 2073 (1996).

[11] D. Umstadter *et al.,* Science **273**, 472 (1996).

[12] J. M. Dawson, Phys. Rev. **113**, 383 (1959).

[13] Y. Ehrlich *et al.,* Phys. Rev. Lett. **77**, 4186 (1996), and references therein.

[14] G. A. Askar'yan *et al.,* JETP Lett. **60**, 241 (1994); S. V. Bulanov *et al.,* Phys. Rev. Lett. **76**, 3562 (1996).

[15] L. Gorbunov, P. Mora, and T. M. Antonsen, Jr., Phys. Rev. Lett. **76**, 2495 (1996).

[16] A. Pukhov and J. Meyer-ter-Vehn, Phys. Rev. Lett. **76**, 3975 (1996).

[17] A. Gray, in *Modern Differential Geometry of Curves and Surfaces* (CRC Press, London, 1993), p. 95.

[18] V. I. Arnold, *The Theory of Singularities and Its Applications* (Scuola Normale Superiore, Pisa, 1991); T. Poston and Y. Steward, *Catastrophe Theory and its Applications* (Pitman, London, 1978).